Am J Physiol Heart Circ Physiol
280: H2126–H2135, 2001.

Oxidative burst and NO generation as initial response to ischemia in flow-adapted endothelial cells

YEFIM MANEVICH, ABU AL-MEHDI, VLADIMIR MUZYKANTOV, AND ARON B. FISHER
Institute for Environmental Medicine, University of Pennsylvania Medical Center, Philadelphia, Pennsylvania 19104-6068

Received 28 September 2000; accepted in final form 15 December 2000

Manevich, Yefim, Abu Al-Mehdi, Vladimir Muzykantov, and Aron B. Fisher. Oxidative burst and NO generation as initial response to ischemia in flow-adapted endothelial cells. *Am J Physiol Heart Circ Physiol* 280: H2126–H2135, 2001.—Shear stress modulates endothelial physiology, yet the effect(s) of flow cessation is poorly understood. The initial metabolic responses of flow-adapted bovine pulmonary artery endothelial cells to the abrupt cessation of flow (simulated ischemia) was evaluated using a perfusion chamber designed for continuous spectroscopy. Plasma membrane potential, production of reactive O_2 species (ROS), and intracellular Ca^{2+} and nitric oxide (NO) levels were measured with fluorescent probes. Within 15 s after flow cessation, flow-adapted cells, but not cells cultured under static conditions, showed plasma membrane depolarization and an oxidative burst with generation of ROS that was inhibited by diphenyleneiodonium. EGTA-inhibitable elevation of intracellular Ca^{2+} and NO were observed at ~30 and 60 s after flow cessation, respectively. NO generation was decreased in the presence of inhibitors of NO synthase and calmodulin. Thus flow-adapted endothelial cells sense the altered hemodynamics associated with flow cessation and respond by plasma membrane depolarization, activation of NADPH oxidase, Ca^{2+} influx, and activation of Ca^{2+}/calmodulin-dependent NO synthase. This signaling response is unrelated to cellular anoxia.

reduced nicotinamide adenine dinucleotide phosphate oxidase; plasma membrane potential; shear stress; intracellular calcium; O_2 consumption

ENDOTHELIAL CELLS exposed to blood flow are thought to have mechanosensors that convert shear stress-related mechanical forces in the plasma membrane into specific cellular signaling system(s) (4, 7, 10, 14). This paradigm has been studied predominantly with endothelial cells subjected to increasing levels of shear, whereas the effect(s) of decreased shear is relatively poorly characterized or understood. In ischemia (e.g., a vessel occlusion), flow cessation is generally followed by hypoxia and cultured cells subjected to hypoxia have been used as a model for ischemia (28, 29). However, the response to hypoxia alone cannot adequately model the endothelial response to the mechanical component of ischemia. Furthermore, endothelial cells are normally preconditioned to flow and their ability to sense and respond to ischemia may differ from the responses of static cells that are known to lose certain endothelial-specific features (e.g., caveoli and cytoskeleton organization) when removed from the circulation (10, 11, 21).

We previously used imaging techniques in an isolated rat lung model, continuously ventilated to maintain oxygenation, to separate ischemia from hypoxia and to detect pulmonary endothelial responses to loss of shear stress in situ. Based on measurements with fluorescent dyes, flow cessation resulted in depolarization of the endothelial plasma membrane, generation of reactive O_2 species (ROS) and increase in intracellular Ca^{2+} concentration ($[Ca^{2+}]_i$) (1, 3, 25). To isolate the response by endothelial cells from that due to other cell types in the tissue and to assess this paradigm in a more generic endothelial cell type, we expanded these studies to an in vitro system of endothelial cells preadapted to flow in artificial capillaries. This latter study showed that flow cessation (simulated ischemia) results in increased ROS generation, activation of nuclear factor-κβ (NF-κβ) and activator protein-1, and subsequent cellular proliferation (27). However, this in vitro artificial capillary system could not be used to detect and quantitate the initial responses to ischemia in real time kinetics because the artificial capillaries are opaque and direct observation of cells by microscopy or spectroscopy is not possible. Furthermore, trypsinization was required to detach cells before their study, necessitating a 5- to 10-min delay between the ischemic stimulus and subsequent cellular examination (27).

The goal of the present study was to characterize the initial molecular events after flow cessation in flow-adapted endothelial cells. We designed a laminar-flow, parallel-plate chamber that can be used for flow adaptation and also for the continuous spectroscopic study of an endothelial cell monolayer. This system allowed us to study the initial cellular metabolic events after onset of simulated ischemia. Our results indicate that flow-adapted endothelial cells, but not those cultured under static conditions, respond to flow cessation by an immediate membrane depolarization and powerful ox-

Address for reprint requests and other correspondence: A. B. Fisher, Institute for Environmental Medicine, University of Pennsylvania School of Medicine, 1 John Morgan Bldg., 3620 Hamilton Walk, Philadelphia, PA 19104-6068 (E-mail: watsonj@mail.upenn.edu).

The costs of publication of this article were defrayed in part by the payment of page charges. The article must therefore be hereby marked "*advertisement*" in accordance with 18 U.S.C. Section 1734 solely to indicate this fact.

idative burst, followed by increase in $[Ca^{2+}]_i$ and activation of Ca^{2+}/calmodulin-dependent nitric oxide (NO) synthase.

MATERIALS AND METHODS

Materials. Ferricytochrome *c* (cyt *c*; from horse heart), HEPES, Cu-Zn superoxide dismutase (EC1.15.1.1) (SOD) from bovine erythrocytes, catalase (EC1.11.1.6) from bovine liver, and EGTA were purchased from Sigma (St. Louis, MO). 4,5-Diaminofluorescein (DAF-2) diacetate was purchased from Calbiochem (San Diego, CA). The phosphorescence probe, PdP1, was a gift from Dr. S. Vinogradov, Biochemistry and Biophysics Department of the University of Pennsylvania. Diphenyleneiodonium chloride (DPI) was purchased from ICN Biomedicals (Costa Mesa, CA). Bis-(1,3-dibutylbarbituric acid)trimethine oxonol (bis-oxonol), 2′,7′-dichlorodihydrofluorescein (H_2DCF) diacetate, fura 2-acetoxymethyl ester (AM), *N*-6-aminohexyl-5-chloro-1-naphthalene sulfonamide (W-7), and N^G-nitro-L-arginine methyl ester (L-NAME) were purchased from Molecular Probes (Eugene, OR). Eagle's minimal essential medium (MEM) and other cell culture reagents were purchased from GIBCO BRL (Gaithersburg, MD). Fetal bovine serum (FBS) was purchased from Hyclone (Logan, UT). Pronectin F was purchased from Protein Polymer Technologies (San Diego, CA). Bovine pulmonary artery endothelial cells (BPAEC) were purchased from the American Type Culture Collection (Manassas, VA) at *passage 15*; we have shown previously that these cells show a similar response to ischemia as BPAEC at *passage 3–4* (27).

Laminar flow chamber. A flow chamber with parameters similar to those of a parallel-plate chamber (19) was designed for spectroscopic study of a confluent monolayer of BPAEC after adaptation to laminar flow. BPAEC adherent to a 12.5 × 25 mm quartz or plastic slide (Aclar, Allied Signal; Morristown, NJ) were placed inside the chamber and perfused by using a peristaltic pump (Harvard Apparatus; South Natick, MA) (Fig. 1*A*). A rubber ring gasket was used to channel the flow. Observation of dye added to the perfusate indicated that laminar flow conditions were achieved with flow rates between 0.5 and 9 ml/min. The volume of the chamber perfusion area was 28 μl, and the total volume of the perfusion circuit was ~20 ml. The pump, perfusate reservoir, and chamber were connected with Tygon tubing (1/32 in. ID, 5/32 in. OD, Cole-Parmer Instrument) (Fig. 1). Temperature control (at 37°C) was maintained with a water circulator (model 1104, VWR Scientific). The 10 × 10 mm chamber was made of stainless steel (Fig. 1, *B–D*) with an insulated permanent quartz window and dimensions to fit the standard spectrophotometer/spectrofluorometer sample holder. Its geometry (optical path ~0.35 mm, 45° angle orientation of plastic slide with adherent cells to the direction of excitation beam) was designed for use in a UV-VIS spectrometer or with a light microscope. The plastic slide transmitted ~95% of light at all wavelengths between 220 and 800 nm.

Cell culture and simulated ischemia. Quartz or plastic slides were sterilized with 70% ethanol, air dried in a tissue culture hood, treated for 20 min at 37°C with 1 ml of a 50 μg/ml solution of Pronectin F, and washed twice with MEM. BPAEC were grown on slides placed in a 35-mm tissue culture dish (two identical slides per dish). BPAEC in MEM supplemented with 15% FBS (Hyclone) and 100 U/ml penicillin, 100 μg/ml streptomycin, 1 mM sodium pyruvate, 100 μM of nonessential amino acid solution, and 10 mM HEPES, pH 7.4 were plated at 1×10^6 cells per dish (2 slides) and allowed to grow for 48 h until they became fully confluent. The number of cells per slide at confluence in the perfusion area was ~1×10^5. For adaptation to flow, a slide with adherent cells was perfused in the flow chamber with growth medium supplemented with 25 mM HEPES (pH 7.4) at 37°C generally for 24 h at an estimated shear stress at the cell surface of 5 dyn/cm^2. A similarly prepared slide was maintained under static culture conditions for the same duration (called static cells).

Two hours before an experiment, the flow chamber was placed into the temperature-controlled (37°C) sample holder of a spectrophotometer (or spectrofluorometer), whereas perfusion continued. After 1 h, the growth medium was substituted with a standard Krebs-Ringer buffer (pH 7.4) supplemented with 10 mM glucose plus 25 mM HEPES and perfusion continued for an additional 1 h. Simulated ischemia was induced by abrupt cessation of perfusate flow through the chamber. As shown below, cells became hypoxic in ~4 min after flow cessation and as a result, all studies related to ischemia generally were completed during this time. Cells grown under static conditions were placed in the chamber, perfused for 30 min, and then subjected to abrupt ischemia (static cells control).

Spectroscopic measurements. Superoxide anion radical ($O_2^{\cdot-}$) generation was evaluated by measurement of absorbance of cyt *c* (13) using a Beckman DU 640B (Beckman Instruments; Fullerton, CA) dual beam spectrophotometer (3 nm slits). For detection of $O_2^{\cdot-}$, cyt *c* was added to perfusate to 150 μM final concentration. Reduction of cyt *c* by $O_2^{\cdot-}$ was measured by change in absorbance at 550 nm. Spectra were recorded at 30-s intervals during simulated ischemia or in the real-time kinetic mode with resolution of one point each 15 s.

Fluorescence measurements for intracellular Ca^{2+}, ROS or NO generation, or for endothelial cell membrane potential measurements utilized a PTI spectrofluorometer (Photon Technology International; Bricktown, NJ) equipped with single photon counting system with excitation (Ex) and emission (Em) slits at 1 and 3 nm, respectively. For the measurement of transmembrane potential, we used bis-oxonol added to perfusate at 20 nM final concentration. For ROS, Ca^{2+}, or NO detection, the cell membrane permeable dye (either H_2DCF diacetate, fura 2-AM, or DAF-2 diacetate) was added into the perfusate to 5 μM final concentration. After 30 min, the monolayer of BPAEC was washed twice with fresh perfusate to eliminate extracellular dye. Detection of bis-oxonol fluorescence was at 520 nm (Ex. 490 nm). H_2DCF fluorescence for ROS was measured at 530 nm (Ex. 488 nm). fura 2-AM fluorescence at 510 nm was detected using 340 and 380 nm excitation in the excitation ratio mode (time of excitation wavelength adjustment about 5 s). The ratio of fura 2 emission at both of the excitation wavelengths (I_{340}/I_{380}) was calibrated for known concentrations of Ca^{2+} to estimate $[Ca^{2+}]_i$ (14). For experiments to measure NO production, the perfusate was supplemented with 2 mM arginine. DAF-2 fluorescence for NO was measured at 530 nm (Ex. 490 nm) (18).

The partial pressure of O_2 in the perfusate was measured by phosphorescence of PdP1 (Ex. 524 nm, Em. 690 nm) using a LS 50B luminescence spectrometer (Perkin-Elmer; Buckinghamshire, UK) with 0.15 ms delay time, 0.5 ms gating, 15 ms cycle time, and one flash per cycle. This method results in increasing phosphorescence due to dequenching as O_2 partial pressure in the cells decreases (17, 26). We used the glucose/glucose oxidase (GOX) reaction with the Whalen-Nair O_2 microelectrode to calibrate the Po_2 at which phosphorescence of PdP1 became detectable under our experimental conditions; the decrease in Po_2 was due to utilization of O_2 by GOX to produce H_2O_2. With

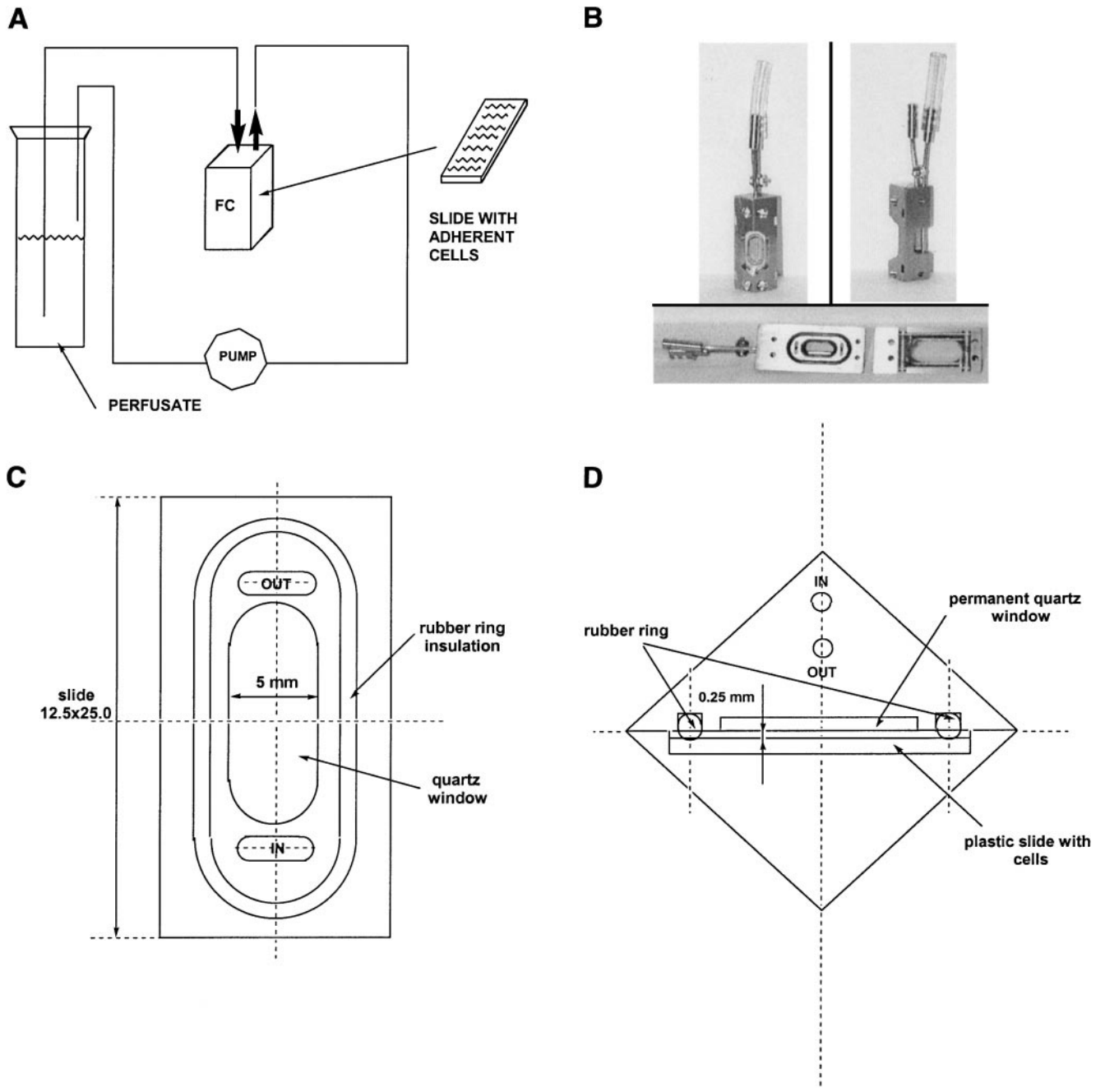

Fig. 1. Details of the perfusion flow chamber (FC) used to adapt cells to flow and to study the initial events after cessation of flow. *A*: scheme of the perfusion circuit showing a slide with confluent monolayer of bovine pulmonary artery endothelial cells (BPAEC) in the laminar FC. The FC and perfusate reservoirs were placed in a temperature-controlled bath. *B*: digitized photograph showing assembled (*top*) and disassembled (*bottom*) FC. *C*: diagonal cross section of flow area of the FC. IN and OUT indicate the perfusion flow path. *D*: top view of horizontal cross section of flow area.

the use of 50 mM glucose and 50 μg/ml GOX in Krebs-Ringer buffer (pH 7.4, 37°C) supplemented with 25 mM HEPES, PdP1 phosphorescence was detected when P_{O_2} decreased to 45 ± 3 Torr (means ± SE for $n = 3$).

Fluorescence microscopy. Slides with flow-adapted BPAEC before or after simulated ischemia were imaged with an epifluorescence microscope with ×100 objective (Nikon Diaphot TMD) and equipped with an optical filter changer (Lambda 10–2, Sutter Instrument). Excitation was accomplished with a mercury lamp with narrow bandpass filter (FITC 485/10), triple-band dichroic mirror (D/F/R-BS&M, Chroma Technolog; Brattleboro, VT), and a narrow bandpass filter (535/40 transmission/half bandwidth, in nm) for emitted light. Images were acquired during a 500-ms exposure with a computer-controlled cooled CCD camera (MicroMAX, Princeton Instruments; Princeton, NJ) using graphics control software (Metamorph Imaging System, Universal Imaging; West Chester, PA). After fluorescence images were acquired, matching phase-contrast images were taken from the same area.

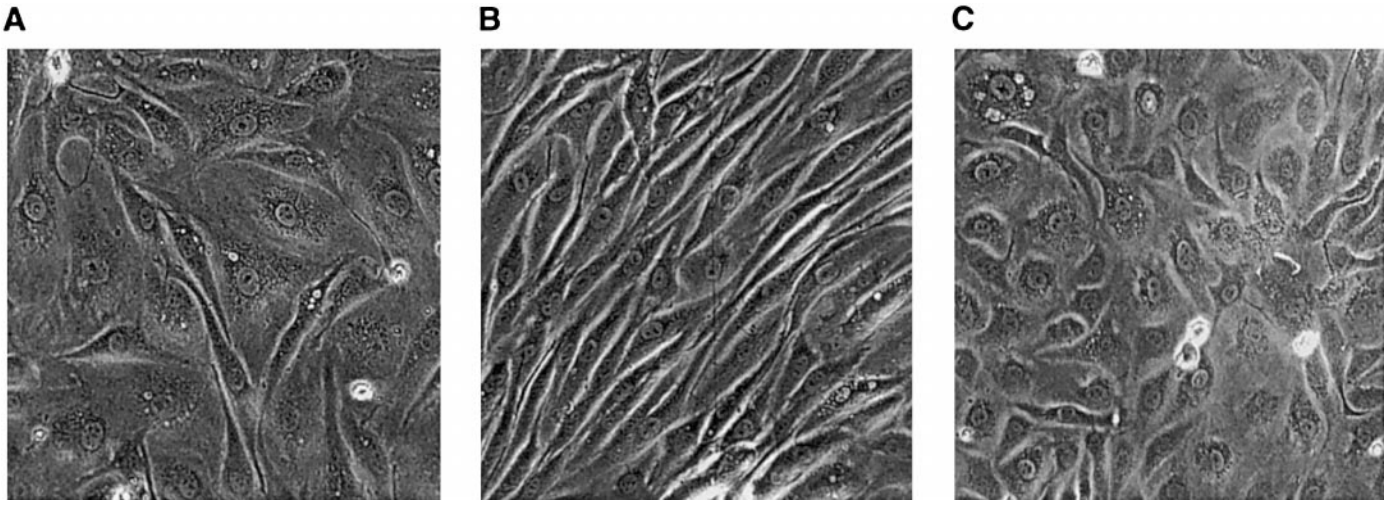

Fig. 2. Phase microscopy of confluent BPAEC in cell culture on a plastic slide. *A*: cells were cultured for 24 h and observed before exposure to laminar flow. *B*: same cells after exposure to laminar flow with shear stress of 5 dyn/cm^2 for 24 h. Cells have aligned in the flow path. *C*: same cells after incubation for an additional 24 h under no flow (static) conditions.

Data analysis. Results are expressed as means ± SE. Curves were fit to original data using KaleidoGraph V.3.0.2 (Synergy Software; Reading, PA) for Macintosh computer using the smoothing procedure, linear or polynomial fit. Iterations were repeated until the correlation coefficient (R) for the fit exceeded 0.9.

RESULTS

Adaptation of a confluent monolayer of BPAEC to laminar flow as described above (shear stress at 5 dyn/cm^2 for 24 h) resulted in the alignment of cells to the direction of flow with reversion to their original shape during an additional 24-h incubation under static (no-flow) culture conditions (Fig. 2). Similar flow-mediated changes in endothelial cell alignment to laminar flow have been reported previously in other experimental systems in vitro (11, 22). This result indicates that our flow chamber was satisfactory for flow adaptation of endothelial cells.

Our previous studies using a membrane potential-sensitive fluorescent probe, bis-oxonol, in the oxygenated perfused rat lung preparation revealed that simulated ischemia caused endothelial plasma membrane depolarization (3). In the present study, flow-adapted BPAEC showed a rapid (within 15 s after onset of ischemia) increase in bis-oxonol fluorescence after cessation of flow compatible with plasma membrane depolarization, and a rapid decrease of bis-oxonol fluorescence after start of reperfusion compatible with repolarization (Fig. 3). There was no change in bis-oxonol fluorescence during simulated ischemia with BPAEC that had not been flow adapted (not shown).

Cells in the chamber are oxygenated by perfusate flow. Therefore, it is expected that P_{O_2} in the medium and cells will decrease with ischemia as a result of O_2 utilization reflecting cellular metabolic activity. In this respect, our system is a model for ischemia in systemic blood vessels. Cellular P_{O_2} was monitored with the phosphorescent probe PdP1 that localizes extracellularly and displays increasing phosphorescence with decreasing perfusate P_{O_2}. A detectable increase in the phosphorescence signal was noted at 4–5 min after flow cessation in the flow-adapted monolayer of BPAEC, indicating that P_{O_2} had decreased to about 45 mmHg (Fig. 4). Saturation of perfusate with 100% O_2 resulted in approximately fivefold prolongation (~20 min) in the time required for detection of increased phosphorescence compatible with the expected approximately fivefold increase in perfusate O_2 content. Cells cultured under static (no flow) conditions showed detectible phosphorescence after ~16 min of ischemia (Fig. 4), indicating a rate of O_2 consumption that was ~25% of that seen with flow-adapted cells.

The high rate of O_2 consumption by the flow-adapted cells is compatible with a powerful oxidative burst triggered by ischemia as indicated by our previous

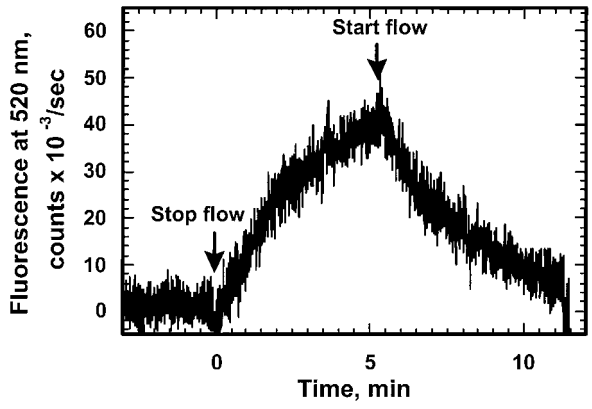

Fig. 3. Cell membrane potential as indicated by bis-oxonol fluorescence. Effect of simulated ischemia (stop flow) and reperfusion (start flow) on bis-oxonol fluorescence in a monolayer of flow-adapted (5 dyn/cm^2, 24 h) BPAEC. Cells were prelabeled with 0.02 μM bis-oxonol and fluorescence was monitored at 520 nm (490 nm excitation). An increase in fluorescence indicates plasma membrane depolarization.

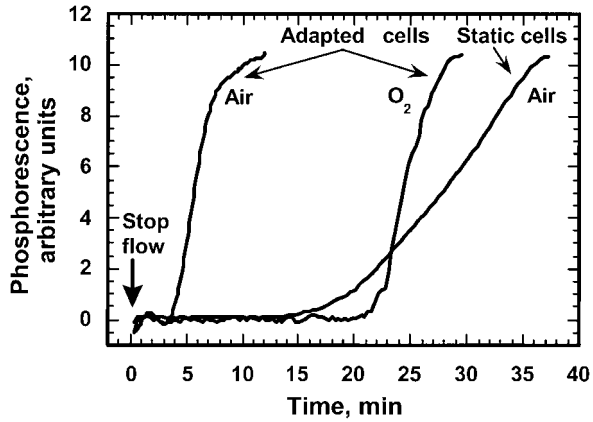

Fig. 4. Medium P_{O_2} as indicated by phosphorescence intensity of the extracellular probe PdP1. Phosphorescence during simulated ischemia with BPAEC is expressed in arbitrary units. The initial increase in phosphorescence above baseline indicates P_{O_2} ~45 ± 3 mmHg, whereas the upper plateau reflects essentially zero P_{O_2} (anoxia). With flow-adapted cells perfused with air-saturated buffer, phosphorescence was undetectable for 4–5 min after flow cessation but then rose rapidly and reached a plateau at ~8 min. When flow-adapted cells were perfused with buffer saturated with O_2, phosphorescence with ischemia remained undetectable for ~20 min and then rose rapidly to a plateau at ~25 min. With static (nonflow adapted) cells perfused with air-saturated buffer, phosphorescence remained at baseline for ~17 min after ischemia and then increased to reach saturation at ~37 min.

studies in the perfused rat lung (29). Cyt *c* was used to detect extracellular $O_2^-\cdot$ generation by the cells. A spectral scan during ischemia demonstrated increasing absorbance maximal at 550 nm, indicating reduction of cyt *c* (Fig. 5*A*). Sodium dithionite was added to the perfusate at the end of each experiment to exclude possible saturation of the signal. Absorbance at 550 nm started to increase within 15 s after flow cessation in flow-adapted cells and reached saturation at ~4 min (Fig. 5*B*). More precise timing within the initial 15-s period was not possible. Similar reduction of cyt *c* ischemia was observed when the external cyt *c* concentration was 75, 100, or 150 μM (data not shown); for subsequent experiments, 150 μM was used to ensure an excess of the detector. No change in absorbance with simulated ischemia was observed with cells cultured under static conditions (Fig. 5*B*). Reduction of cyt *c* was diminished by the addition of SOD to the perfusate and was abolished by preincubation with 20 μM DPI, an inhibitor of flavin-dependent oxidases. Addition of catalase enhanced both the rate and amplitude of cyt *c* reduction during simulated ischemia, suggesting that $O_2^-\cdot$ produced with ischemia is partially dismutated to H_2O_2 that oxidizes cyt *c* and thus attenuates the increase in absorbance. A similar effect of $O_2^-\cdot$ dismutation on cyt *c* absorbance has been observed in experiments with polymorphonuclear leukocytes (24). There was no effect on cyt *c* reduction by preincubation with 1 mM L-NAME for 30 min (data not shown). To evaluate the effect of diminishing perfusate P_{O_2} on the rate of $O_2^-\cdot$ generation, the response to simulated ischemia was measured after saturation of perfusate with 100% O_2. Under these conditions, there was a linear increase

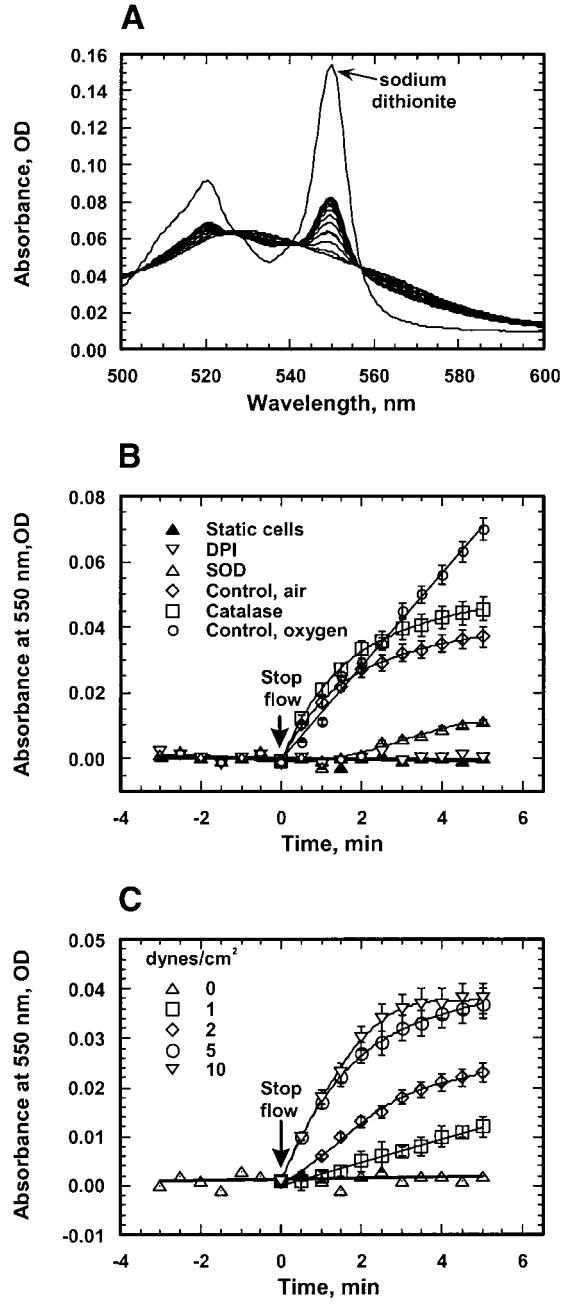

Fig. 5. Extracellular superoxide anion radical ($O_2^-\cdot$) production by BPAEC during simulated ischemia. *A*: effect of simulated ischemia on absorbance spectra of 150 μM ferricytochrome *c* (cyt *c*) added to the perfusate of flow-adapted BPAEC (24 h at 5 dyn/cm²). Spectra were recorded every 30 s after the cessation of flow and showed increasing absorbency at 550 nm with successive scans. The top spectrum was generated by an excess of sodium dithionite added for complete reduction of cyt *c*. The increase of specific absorbance at 550 nm relative to the isosbestic point at 540 nm indicates reduction of cyt *c* by $O_2^-\cdot$. *B*: same conditions as shown in *A* but showing absorbance at 550 nm as a function of time after stopping flow. Conditions are the following: cells that were not flow adapted (static); flow-adapted cells under normoxia (control, air); preperfusion of flow-adapted cells with perfusate saturated with O_2 (control, O_2); preperfusion with diphenyleneiodonium chloride (DPI) (20 μM); and addition of superoxide dismutase (SOD, 20 units) or catalase (25 units) to flow-adapted cells. Results are means ± SE for three independent experiments for each condition. *C*: effect of shear stress magnitude during 24-h adaptation to flow on subsequent $O_2^-\cdot$ generation by BPAEC during simulated ischemia as in *B*. The shear stress during adaptation is indicated as dyn/cm². OD, optical density.

of the cyt *c* absorbance at 550 nm that continued for at least 5 min after cessation of perfusate flow (Fig. 5*B*). Thus the decreasing rate of cyt *c* reduction beginning at about 1.5 min under control conditions likely reflects the increasing limitation of O_2 availability for $O_2^-\cdot$ generation during continuous ischemia.

These studies of simulated ischemia were done with cells adapted for 24 h to a shear stress of 5 dyn/cm^2. To study the effect of shear stress during adaptation on subsequent $O_2^-\cdot$ generation during simulated ischemia, BPAEC were subjected to a level of shear stress between 1 and 10 dyn/cm^2 during the 24-h adaptation period. The rate of $O_2^-\cdot$ generation during simulated ischemia increased progressively with increasing values of shear stress during the prior adaptation period reaching apparent saturation at ~5 dyn/cm^2 (Fig. 5*C*).

The cyt *c* experiments indicated accumulation of $O_2^-\cdot$ in the extracellular compartment. To evaluate whether ROS accumulated intracellularly during simulated ischemia, the fluorophore H_2DCF trapped inside flow-adapted cells was used (2, 27). Within 30 s after onset of simulated ischemia there was a linear increase in fluorescence in flow-adapted cells, indicating H_2DCF oxidation to DCF compatible with increased intracellular ROS. The DCF signal reached a plateau in ~5 min compatible with inhibition of ROS generation due to O_2 depletion (Fig. 6). H_2DCF oxidation with simulated ischemia was markedly inhibited by preperfusion with DPI. H_2DCF oxidation also was markedly inhibited by the presence of catalase in the perfusate (i.e., extracellular). On the other hand, the addition of SOD did not decrease H_2DCF fluorescence, and the tracings suggest a more rapid rate of increase compatible with a more rapid dismutation of $O_2^-\cdot$ to H_2O_2 (Fig. 6). The decrease in DCF fluorescence with ischemia was only modestly inhibited (~18%) by 30-min preincubation of cells with 1 mM L-NAME, indicating that involvement of NO synthase (NOS) in DCF oxidation was relatively minor. There was no increase of DCF fluorescence in cells with simulated ischemia that had not been flow adapted (static cells).

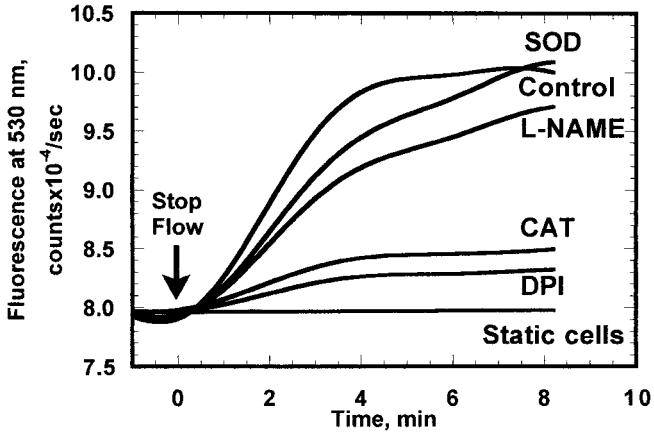

Fig. 6. Intracellular reactive O_2 species (ROS) generation as detected by 2′,7′-dichlorofluorscein (DCF) fluorescence. DCF fluorescence was measured at 530 nm (488 nm excitation) in a monolayer of flow-adapted BPAEC (5 dyn/cm^2, 24 h) during simulated ischemia. Cells were prelabeled by perfusion with 5 μM 2′,7′-dichlorodihydrofluorescein (H_2DCF) diacetate. Conditions were the following: nonflow adapted (static) cells; cells perfused under control conditions; cells preperfused for 30 min with 20 μM DPI or 1 mM N^G-nitro-L-arginine methyl ester (L-NAME); and addition of 25 units catalase (CAT) or of 20 units SOD to the perfusate.

Our previous studies documented that simulated ischemia causes $[Ca^{2+}]_i$ elevation in the pulmonary endothelium of the isolated lung (21). We characterized the kinetics of $[Ca^{2+}]_i$ changes in flow-adapted BPAEC during the ischemic episode using the fluorophore fura 2. The level of resting $[Ca^{2+}]_i$ in flow-adapted cells was ~135 nM. It began to increase ~30 s after flow cessation in flow-adapted, but not static, cells and reached a maximum level of 270 nM within 10 min (Fig. 7). The increase was markedly inhibited by the addition of EGTA (3 mM) to the perfusate. In contrast, preperfusion with the calmodulin inhibitor W-7 resulted in acceleration and elevation of amplitude of $[Ca^{2+}]_i$ response to ischemia in flow-adapted cells likely due to reduction in capacity of calmodulin to buffer $[Ca^{2+}]_i$.

Elevation of $[Ca^{2+}]_i$ is known to activate the endothelial NOS isoform via a calmodulin-dependent mechanism (16). We therefore studied NO generation during simulated ischemia in flow-adapted cells using detection of intracellular NO by a plasma membrane-permeable, NO-specific fluorescent dye, DAF-2 diacetate. Preincubation of BPAEC with 5 μM DAF-2 diacetate for 30 min resulted in trapping of deacetylated dye in the cells. This probe becomes highly fluorescent after reaction with NO (18). There was a linear increase in DAF-2 fluorescence in flow-adapted, but not static, cells that began ~50 s after flow cessation (Fig. 8) indicating intracellular NO generation. NO generation was abolished by the NOS inhibitor L-NAME and inhibited ~50% by the calmodulin inhibitor W-7. When the perfusate was saturated with 100% O_2, NO generation with ischemia remained linear during 5 min (Fig. 8).

Imaging of flow-adapted BPAEC preloaded with H_2DCF diacetate or DAF diacetate fluorescent probes in a fluorescence microscope showed that simulated ischemia results in a marked increase in cytoplasmic fluorescence intensity of both fluorophores (Fig. 9) as expected from the spectroscopic measurements.

DISCUSSION

Endothelial responses to flow alterations via mechanosensor elements may represent a fundamental physiological paradigm. However, the response(s) to ischemia remain(s) to be more fully characterized and understood. In many settings, ischemia (flow cessation) leads to hypoxia and, therefore, the responses to mechanical signal(s) may become rapidly overshadowed by those related to a low O_2 level. Therefore, identification of the initial molecular and cellular events caused by flow cessation in endothelial cells represents an important and challenging goal. Our present study characterized the initial metabolic responses of flow-adapted endothelial cells to ischemia under conditions of adequate oxygenation. Adequate

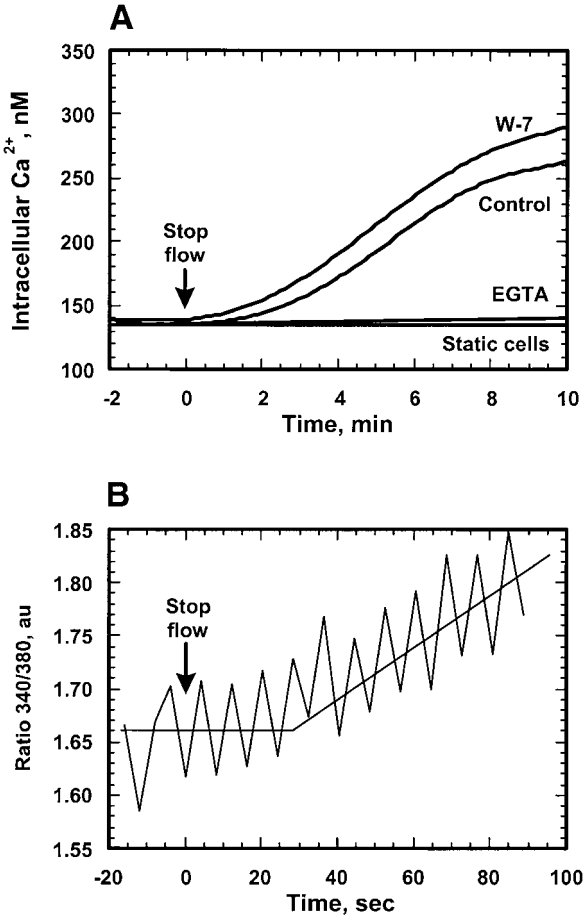

Fig. 7. Intracellular Ca^{2+} measured by fura 2-acetoxymethyl ester (AM) fluorescence. Flow-adapted BPAEC were prelabeled with 5 μm fura 2-AM and fluorescence was measured during simulated ischemia (cessation of flow at *time 0*). Fluorescence at 510 nm was recorded in the ratiometric mode with excitation at 340 and 380 nm. *A*: real time kinetics of intracellular Ca^{2+} concentration ($[Ca^{2+}]_i$). These results were generated using a curve smoothing program (see MATERIALS AND METHODS). The curves on this panel correspond to: static (nonflow adapted) cells; control (flow-adapted) cells; 3 mM EGTA added to perfusate of flow-adapted cells; preperfusion of flow-adapted cells with 25 μM W-7. *B*: recording of the initial response (90 s after onset of ischemia) presented without curve smoothing and showing a resolution for this technique of ~5 s. The saw tooth pattern is produced by movement of the excitation monchromator in the ratio mode between 340 and 380 nm. The linear regression (straight line fit) of data before and after induction of simulated ischemia indicates a delay of ~30 s between the onset of ischemia and the rise of intracellular Ca^{2+}. au, Arbitrary units.

oxygenation was ensured by limiting observations to the initial several min of ischemia when P_{O_2} remained >45 mmHg, the physiological mixed venous P_{O_2}. Adequacy of oxygenation during this period was confirmed by the demonstration of similar effects in air-saturated and O_2-saturated buffers.

Our previous studies using isolated, continuously ventilated rat or mouse lungs have shown that abrupt cessation of pulmonary perfusion causes rapid depolarization of the endothelial plasma membrane, generation of ROS, and increased $[Ca^{2+}]_i$ (1–3, 25). It is important to note that these effects are not a result of reperfusion and that anoxia/reoxygenation is not involved in this model because continuous ventilation maintains adequate oxygenation during lung ischemia and tissue ATP content does not change (3). Ischemia-mediated generation of ROS via a DPI-inhibitable oxidase(s) was confirmed with an in vitro system using flow-adapted BPAEC in artificial capillaries (27). Lung endothelium contains multiple DPI-inhibitable oxidases such as xanthine oxidase, mitochondrial NADH dehydrogenase, cytochrome *P*-450, and NO synthase that could contribute to ROS generation. Studies in perfused mouse lungs showed that "knock out" of $gp91^{phox}$ eliminated the ROS response to ischemia providing evidence that a phagocyte-type NADPH oxidase is the responsible enzyme (2). Generation of $O_2^{-}\cdot$ outside the cell provides additional evidence that a plasma membrane-associated enzyme is responsible.

The present study utilized an original experimental model permitting direct spectroscopic study in real time or microscopic imaging of flow-adapted cells. Like the previous in vitro model using artificial capillaries (27), we found that adaptation to laminar flow was required to prime the response to simulated ischemia. The most likely mechanism for adaptation is upregulation of shear stress-sensitive elements during the adaptation period, although the specific sensor remains to be identified. Because cellular oxygenation is dependent on perfusate flow in the flow chamber that was utilized in the present study, this system approximates the effect of flow cessation in systemic vessels. Thus O_2 consumption by the cells led to a decrease in P_{O_2} to $<45 \pm 3$ mmHg in about 4–5 min, although this period could be prolonged by perfusion with O_2-equilibrated buffer. Cellular changes with simulated ischemia were sufficiently rapid that they could be readily observed before O_2 limitation. Our results therefore show that endothelial cells adapted to flow as expected with vessels in vivo manifest an O_2-independent response to ischemia before the development of limiting hypoxia.

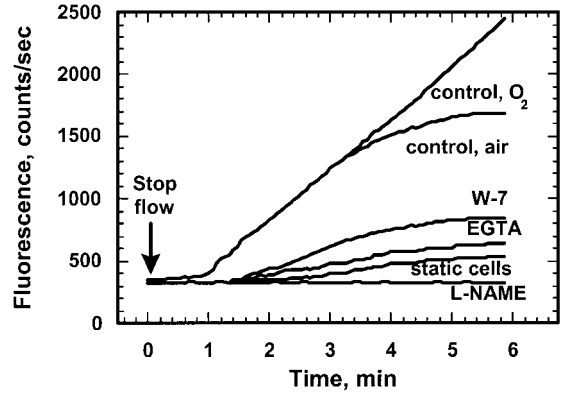

Fig. 8. Nitric oxide (NO) generation measured by diaminofluorescein (DAF-2) fluorescence. Flow-adapted BPAEC were prelabeled by perfusion with 5 μM DAF-2 diacetate. The curves indicate the following: static (nonflow adapted) cells with no additions; control cells (flow-adapted with no additions); cells perfused with O_2-saturated perfusate; preincubation with 1 mM L-NAME; preperfusion for 30 min with 25 μM W-7.

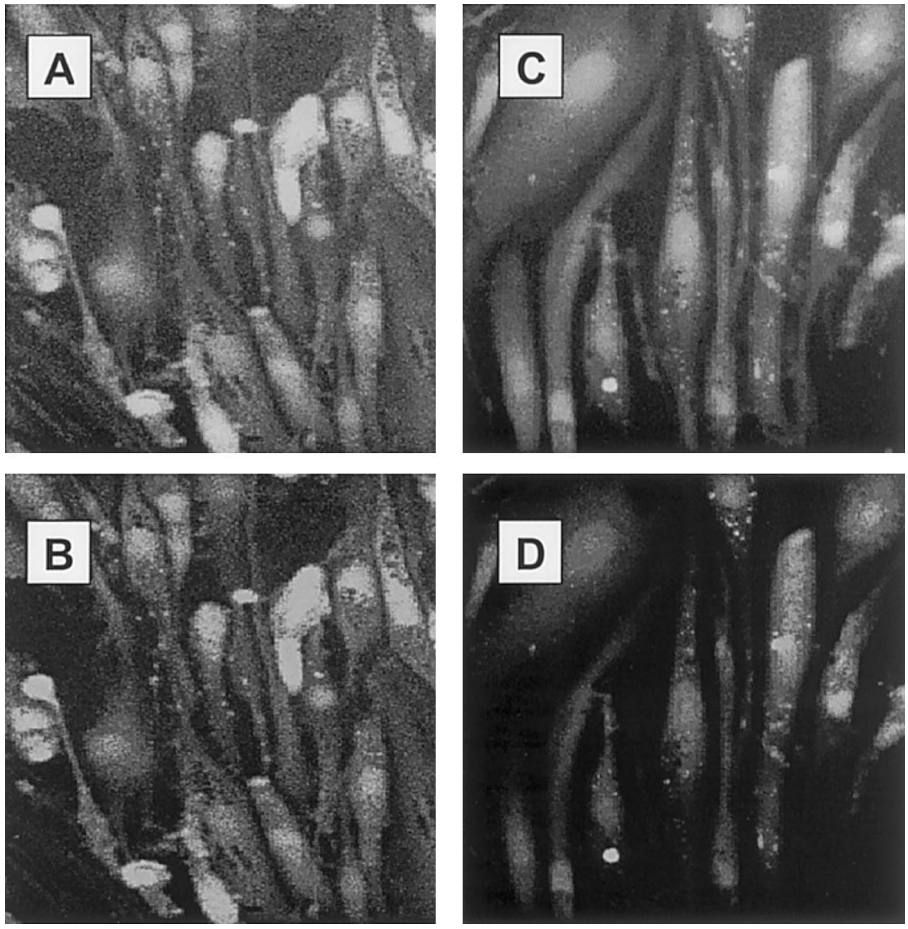

Fig. 9. Fluorescence microscopy for ROS and NO. Effect of simulated ischemia on fluorescent images of flow-adapted BPAEC loaded with H_2DCF (*A* and *B*) or DAF (*C* and *D*). *B* and *D* were obtained with continuously perfused cells and *A* and *C* at 7 min after cessation of flow. The intense fluorescence in *A* and *C* indicates generation of ROS and NO, respectively, with simulated ischemia.

The complex response of endothelial cells to ischemia occurs only in flow-adapted cells and is characterized by a reproducible sequence of events. Within 15 s after flow cessation, depolarization of the plasma membrane occurs and is associated with increased generation of ROS as indicated by reduction of extracellular cyt *c* and by oxidation of the intracellular fluorescent indicator H_2DCF. Extracellular generation of $O_2^-\cdot$ is consistent with the presumed localization of NADPH oxidase to the plasma membrane as has been demonstrated for neutrophils and macrophages (13). Dismutation of extracellular $O_2^-\cdot$ perhaps catalyzed by extracellular SOD on the external plasma membrane (20) will generate H_2O_2. Subsequent diffusion of H_2O_2 into cells would lead to intracellular oxidation of H_2DCF, although other intracellular sources of ROS cannot be excluded. Increased $[Ca^{2+}]_i$ is a subsequent event (starting at about 30 s postischemia) followed by an increase in generation of NO (starting about 1 min postischemia). Thus the present study documents that simulated ischemia in flow-adapted BPAEC leads to endothelial plasma membrane depolarization and a respiratory burst followed by Ca^{2+} influx and increased generation of NO.

As noted above, O_2 consumption by the cells in the present experiments resulted in progressively decreasing O_2 availability. Phosphorescence of the medium was measured continuously during ischemia using the probe PdP1 that shows a detectable increase when P_{O_2} reaches a level of 45 ± 3 Torr. This enabled the calculation of O_2 consumption by the cells. Under standard conditions (37°C, P 760 mmHg, pH 7.4), the O_2 concentration in air-saturated perfusate (Krebs-Ringer bicarbonate) is 0.220 mM and a P_{O_2} of 45 mmHg corresponds to an O_2 concentration of ~0.066 mM. P is the normal pressure of 1 atmosphere. The volume of the chamber is 28 μl and contains ~10^5 cells. Phosphorescence of PdP1 becomes detectable in ~5 min after induction of stimulated ischemia (Fig. 3). Assuming that ischemia results in a linear decrease of O_2 tension in the medium, the mean rate of O_2 consumption for the flow-adapted cells would be the following

$$d[O_2]/dt = (1.54 \times 10^{-4}\ \text{mol/l})(2.8 \times 10^{-5}\ \text{l})/$$
$$(5\ \text{min})(1 \times 10^{-5}\ \text{cells}) = 8.6\ \text{nmol/min per}\ 10^6\ \text{cells}$$

The estimated O_2 consumption for flow-adapted cells in 100% O_2-saturated medium was approximately the same. The estimated mean value for O_2 consumption of static cells in the present experiments is 2.5 nmol/min per 10^6 cells, which is in the same range as the value previously reported for endothelial cells from porcine thoracic aorta in static culture (8). The relative values for O_2 consumption by the cells is qualitatively apparent from the slopes of the phosphorescence plots versus time after medium P_{O_2} reached the point of phospho-

rescence increase (Fig. 4), although we considered quantitation more reliable using the earlier time points (between start of ischemia and initial increase in phosphorescence) when oxygenation was adequate.

Extracellular generation of $O_2^-\cdot$ was detected by reduction of the cell impermeable protein cyt *c*. Using Beers′ law, we can calculate the concentration (C) of cyt *c* reduced by $O_2^-\cdot$ in the chamber during simulated ischemia. This value is equal to $O_2^-\cdot$ production because 1 mole of $O_2^-\cdot$ reduces 1 mole of cyt *c*

$$C = \Delta OD/(\text{ext coeff} \cdot \text{optical path length})$$
$$= 0.013\ \text{min}^{-1}/(21.0\ \text{mM}^{-1} \cdot \text{cm}^{-1} \cdot 0.035\ \text{cm})$$
$$= 0.018\ \text{mM/min}$$

where the change in optical density (ΔOD) between 0 and 2 min is 0.013 per min; the extinction coefficient of cyt *c* is 21.0 $mM^{-1}\cdot cm^{-1}$ (15); and the optical path length is 0.035 cm. Because the chamber volume is 28 μl and contains 10^5 cells, the amount of $O_2^-\cdot$ produced during the initial 2 min of simulated ischemia by BPAEC is 5.1 nmol/min per 10^6 cells. This may underestimate $O_2^-\cdot$ production because of rapid dismutation of $O_2^-\cdot$ (thus escaping the cyt *c* trap) and reoxidation of cyt *c* by H_2O_2. In the presence of catalase in the perfusate, the estimated rate of $O_2^-\cdot$ generation is ~6.1 nmol/min per 10^6 cells. Thus $O_2^-\cdot$ generation accounts for ~70% of O_2 consumption by adapted BPAEC during ischemia, and the respiratory burst accounts for the entire increase in O_2 consumption for the flow-adapted, compared with static, cells. This estimated value for $O_2^-\cdot$ production by the confluent monolayer of flow-adapted BPAEC during simulated ischemia is similar to that seen during the respiratory burst of stimulated neutrophils (4–10 nmol/min per 10^6 cells) (5, 9) and is markedly greater than seen with human umbilical vein endothelial cells simulated by interleukin-1 or recombinant interferon-γ (~0.4 nmol/min per 10^6 cells) (24).

NADPH oxidase, as studied most extensively in phagocytes, is a multicomponent system consisting of both membrane-bound and cytosolic proteins. The rate-limiting step for NADPH oxidase activation is the assembly of these components on the inner leaf of the plasma membrane. In neutrophils, there is a significant lag period for $O_2^-\cdot$ generation after a stimulus such as digitonin (9). The rapid onset of $O_2^-\cdot$ generation after flow cessation (ischemia) in BPAEC suggests preassembly, at least in part, of the NADPH oxidase complex. Transmembrane electron transport via NADPH oxidase could couple with plasma membrane depolarization as observed with these cells, because transmembrane electron transfer provides an actual electrical current. Thus cessation of flow may trigger at least two fast membrane-associated events: inactivation of flow-sensitive K^+ channels leading to membrane depolarization and an electron flux from cytosol to outside of the cells due to NADPH oxidase activation. These two fast-responding membrane-associated systems are coupled and might serve as the effector part of a mechanosensor and signaling mechanism for flow-adapted endothelial cells.

The present results show NO production during simulated ischemia with inhibition by L-NAME, suggesting activation of NOS as a secondary cellular response to flow cessation. The ~45-s delay between membrane depolarization and NO generation could reflect the time required for increase of $[Ca^{2+}]_i$ and subsequent activation of NOS through a Ca^{2+}-dependent, calmodulin-mediated mechanism as indicated by results with EGTA and the calmodulin inhibitor W-7. The dependence of NO generation on Ca^{2+} and calmodulin suggest that endothelial NOS (eNOS) is the responsible isoform for the major fraction of NO production (23). A small amount of NO generation in the presence of EGTA could represent activation, in addition, of the Ca^{2+}-independent NOS isoform previously reported by others (12). The channel responsible for Ca^{2+} influx in these cells remains to be identified. It is generally accepted that cultured endothelial cells do not have voltage-gated Ca^{2+} channels. However, voltage-gated Ca^{2+} channels have been described for freshly isolated capillary endothelial cells (6) suggesting their presence in vivo and raising the possibility that they are induced in endothelium during flow adaptation.

In summary, we have characterized the initial (0–2 min) response of endothelial cells to simulated ischemia during the period of adequate cellular oxygenation. Our results emphasize the fundamental difference in biology of endothelial cells flow adapted (the normal in vivo condition) or maintained in static culture (the artificial or pathological condition). Specifically, flow-adapted, but not static, endothelial cells are capable of sensing flow cessation and respond with ROS generation at an initial rate close to that of the respiratory burst in leukocytes. The subsequent responses include Ca^{2+} influx and increased generation of NO. Thus vascular endothelium can respond to the mechanical component of ischemia via complex biochemical signaling pathways.

We thank William Pennie for constructing the flow chamber, Dr. Stephen Thom for use of the luminescence spectrometer, Dr. S. Vinogradov for the gift of PdP1, Drs. D. Buerk and F. Bronco for help with PdP1 calibration, Kristine DeBolt for help with BPAEC culture, Maggie Meuler for assistance with assays, and Elaine Primerano for typing the manuscript.

This work was supported by National Heart, Lung, and Blood Institute Grant HL-60290.

REFERENCES

1. **Al-Mehdi AB, Shuman H, and Fisher AB.** Intracellular generation of reactive oxygen species during nonhypoxic lung ischemia. *Am J Physiol Lung Cell Mol Physiol* 272: L294–L300, 1997.
2. **Al-Mehdi AB, Zhao G, Dodia C, Tozawa K, Costa K, Muzykantov V, Ross C, Blecha F, Dinauer M, and Fisher AB.** Endothelial NADPH oxidase as the source of oxidants in lungs exposed to ischemia or high K^+. *Circ Res* 83: 730–737, 1998.
3. **Al-Mehdi AB, Zhao G, and Fisher AB.** ATP-independent membrane depolarization with ischemia in the oxygen-ventilated isolated rat lung. *Am J Respir Cell Mol Biol* 18: 653–661, 1997.
4. **Barakat AL, Leaver EV, Pappone PA, and Davies PF.** A flow-activated chloride-selective membrane current in vascular endothelial cells. *Circ Res* 85: 820–828, 1999.

5. **Bellavite P.** The superoxide-forming enzymatic system of phagocytes. *Free Rad Biol Med* 225–261, 1988.
6. **Bossu JL, Feltz A, Rodeau JL, and Tanzi F.** Voltage-dependent transient calcium currents in freshly dissociated capillary endothelial cells. *FEBS Lett* 255: 377–380, 1989.
7. **Chien S, Li S, and Shyy YJ.** Effects of mechanical forces on signal transduction and gene expression in endothelial cells. *Hypertension* 31: 162–169, 1998.
8. **Clementi E, Brown GG, Foxwell N, and Moncada S.** On the mechanism by which vascular endothelial cells regulate their oxygen consumption. *Proc Natl Acad Sci USA* 96: 1555–1562, 1999.
9. **Cohen HJ and Chovaniec ME.** Superoxide generation by digitonin-stimulated guinea pig granulocytes. *J Clin Invest* 61: 1081–1087, 1978.
10. **Davies PF.** Flow-mediated endothelial mechanotransduction. *Physiol Rev* 75: 519–560, 1995.
11. **Dewey CF, Bussolari SR, Gimbrone MA, and Davies PF.** The dynamic response of vascular endothelial cells to fluid shear stress. *J Biomed Eng* 103: 177–185, 1981.
12. **Dimmeler S, Fleming L, Fisslthaler B, Hermann C, Busse R, and Zeiher AM.** Activation of nitric oxide synthase in endothelial cells by Akt-dependent phosphorylation. *Nature* 399: 601–605, 1999.
13. **Griendling KK, Sorescu D, and Ushio-Fukai M.** NAD(P)H oxidase: role in cardiovascular biology and disease. *Circ Res* 86: 494–501, 2000.
14. **Grynkiewicz G, Poenie M, and Tsien RY.** A new generation of Ca^{2+} indicators with greatly improved fluorescent properties. *J Biol Chem* 260: 33440–3452, 1985.
15. **Jones OTG and Hancock JT.** Assays of plasma membrane NADPH oxidase. *Methods Enzymol* 233: 223–225, 1994.
16. **Kuchan MJ and Frangos JA.** Role of calcium and calmodulin in flow-induced nitric oxide production in endothelial cells. *Am J Physiol Cell Physiol* 266: C628–C636, 1994.
17. **Lo LW, Vinogradov SA, Koch CJ, and Wilson DF.** A new, water soluble, phosphor for oxygen measurements in vivo. *Adv Exp Med Biol* 428: 651–656, 1997.
18. **Nakatsubo N, Kojima H, Kikuchi K, Nagoshi H, Hirata Y, Maeda D, Imai Y, Irimura T, and Nagano T.** Direct evidence of nitric oxide production from bovine aortic endothelial cells using new fluorescence indicators: diaminofluoresceins. *FEBS Lett* 427: 263–266, 1998.
19. **Nauman E, Risic KJ, Keaveny TM, and Satcher RL.** Quantitive assessment of steady and pulsatile flow fields in a parallel plate flow chamber. *Ann Biomed Eng* 27: 194–199, 1999.
20. **Oury TD, Day BJ, and Crapo JD.** Extracellular superoxide dismutase in vessels and airways of humans and baboons. *Free Radic Biol Med* 20: 957–965, 1996.
21. **Rizzo V, McIntosh DP, Oh P, and Schnitzer JE.** In situ flow activates endothelial nitric oxide synthase in luminal caveolae of endothelium with rapid caveolin dissociation and calmodulin association. *J Biol Chem* 273: 34724–34729, 1998.
22. **Satcher R, Dewey CF, and Hartwig JH.** Mechanical remodeling of the endothelial surface and actin cytoskeleton induced by fluid flow. *Microcirculation* 4: 439–453, 1997.
23. **Stuehr DJ.** Mammalian nitric oxide synthases. *Biochim Biophys Acta* 1411: 217–230, 1999.
24. **Tauber AI and Babior BM.** $O_{\bar{2}}$ and host defense: the production and fate of $O_{\bar{2}}$ in neutrophils. *Photochem Photobiol* 28: 701–709, 1978.
25. **Tozawa K, Al-Mehdi AB, Muzykantov V, and Fisher AB.** In situ imaging of intracellular calcium with ischemia in lung subpleural microvascular endothelial cells. *Antioxid Redox Signaling* 1: 145–153, 1999.
26. **Vinogradov SA and Wilson DF.** "Dendritic" porphyrins. New protected phosphors for oxygen measurements in vivo. *Adv Exp Med Biol* 428: 657–662, 1997.
27. **Wei Z, Costa K, Al-Mehdi AB, Dodia C, Muzykantov V, and Fisher AB.** Simulated ischemia in flow-adapted endothelial cells leads to generation of reactive oxygen species and cell signaling. *Circ Res* 85: 682–689, 1999.
28. **Young W and Block ER.** Effect of hypoxia and reoxygenation on the formation and release of reactive oxygen species by porcine pulmonary artery endothelial cells. *J Cell Physiol* 164: 414–423, 1995.
29. **Zulueta JJ, Sawhney R, Yu FS, Cote CC, and Hassoun PM.** Intracellular generation of reactive oxygen species in endothelial cells exposed to anoxia-reoxygenation. *Am J Physiol Lung Cell Mol Physiol* 272: L897–L902, 1997.